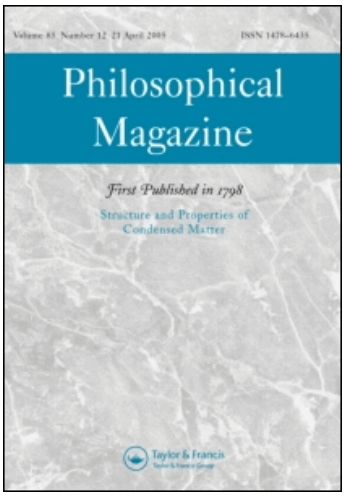

Philosophical Magazine
Publication details, including instructions for authors and subscription information:
http://www.informaworld.com/smpp/title~content=t713695589

Finite element simulation and experimental determination of interfacial adhesion properties by wedge indentation

L. Chen [ab]; K. B. Yeap [a]; K. Y. Zeng [a]; G. R. Liu [bc]
[a] Department of Mechanical Engineering, National University of Singapore, Singapore [b] Centre for Advanced Computations Engineering Science (ACES), National University of Singapore, Singapore [c] National University of Singapore, Singapore

Online Publication Date: 01 June 2009

To cite this Article Chen, L., Yeap, K. B., Zeng, K. Y. and Liu, G. R.(2009)'Finite element simulation and experimental determination of interfacial adhesion properties by wedge indentation',Philosophical Magazine,89:17,1395 — 1413
To link to this Article: DOI: 10.1080/14786430902973858
URL: http://dx.doi.org/10.1080/14786430902973858

Philosophical Magazine
Vol. 89, No. 17, 11 June 2009, 1395–1413

Taylor & Francis
Taylor & Francis Group

Finite element simulation and experimental determination of interfacial adhesion properties by wedge indentation

L. Chen[ab], K.B. Yeap[a], K.Y. Zeng[a]* and G.R. Liu[bc]

[a]*Department of Mechanical Engineering, National University of Singapore, 9 Engineering Drive 1, 117576 Singapore;* [b]*Centre for Advanced Computations Engineering Science (ACES), National University of Singapore, 9 Engineering Drive 1, 117576 Singapore;* [c]*National University of Singapore, Singapore–MIT Alliance (SMA), E4-04-104, Engineering Drive 3, 117576 Singapore*

(*Received 23 October 2008; final version received 10 April 2009*)

This paper presents our recent study on determination of interfacial adhesion properties of soft-film-on-hard-substrate (SFHS) systems using finite element simulation (FEM) and wedge indentation experiments. The objectives of this study are: (i) to simulate the interfacial delamination processes during wedge indentation experiments; (ii) to study the effects of interfacial delamination on the characteristics of the indentation load–displacement (P–h) curves, (iii) to determine the interfacial adhesion properties; and (iv) to compare the simulation and experimental results. During the FEM simulation, a traction-separation law is used to describe the interfacial adhesion properties due to the large-scale yielding during indentations. The effects of main parameters in the traction-separation law, i.e. interfacial strength and interfacial energy, to the initiation of interfacial delamination are studied by parametric studies. An interface energy-strength contour, which can be used to determine the interfacial adhesion properties of the thin-film/substrate systems based on a wedge indentation experiment, is developed from the outcomes of the FEM simulation of the indentations using wedge tips with the inclusion angles of 90° and 120°. Using the respective interface energy-strength contours, the interfacial energy and strength of a BlackDiamond® (BD)/Si system and a methylsilsesquioxane (MSQ)/Si system are determined. The simulated results are then compared with the previous experimentally derived interfacial fracture toughness values and some further discussions are given.

Keywords: wedge indentation; adhesion; cohesive zone model; computer simulation; films; finite-element modeling; indentation; interfaces

1. Introduction

Thin-film systems are widely used in many technologically important applications, including microelectronic and optoelectronic devices, magnetic data storage and medical devices. An important issue in all thin-film/substrate systems is the reliability of the interface between film and substrate, since interfacial failure may lead to a

*Corresponding author. Email: mpezk@nus.edu.sg

ISSN 1478–6435 print/ISSN 1478–6443 online

DOI: 10.1080/14786430902973858
http://www.informaworld.com

system failure even though the film and substrate still satisfy technical requirements; this issue has, therefore, attracted a great deal of attention in recent years [1–7].

Nano-indentation techniques, such as spherical, conical or wedge indentation, have proven very effective in the investigation of interfacial delamination of film systems [6–20]. During indentations, the interfacial delamination can be reflected and identified by characteristic changes in the indentation load–displacement curves (*P–h* curves). Marshall and Evans [10] provided a basis for utilizing indentation methods to evaluate fracture toughness or coherency of interfaces in thin-film systems. They used an indentation experiment to measure the interfacial adhesion properties of ZnO/Si system [11]. Swain and Mencik [12] demonstrated various responses in the indentation load–displacement curves caused by interfacial delamination during spherical indentations. Drory and Hutchinson [13] also used a conical indentation method to assess interface toughness. Recently, wedge indentation methods have been used extensively [6–9,14–16]. Yeap et al. [19,20] adapted a wedge indentation method and focused-ion-beam (FIB) technique to determine the interfacial toughness of a low dielectric constant (low k) film on a silicon substrate. However, most of these studies did not measure interfacial strength, i.e. the maximum stress to separate an interface. In addition, it was assumed that the indentation plastic zone was incompressible and was confined to the region near the indenter tip [10–20]. However, as will be shown in this study, the entire region of the film above the crack at the interface was found to be yielding during FEM (finite element method) simulation; thus, interfacial toughness may be overestimated due to the disturbance of plastic dissipation energy. Therefore, it is necessary to use a numerical method to study the large-scale yielding behavior during indentation so that the interfacial adhesion properties can be accurately derived.

With reference to simulating wedge indentation experiments characterizing the interfacial properties of thin films, Zhang et al. [21] employed a traction-separation law (cohesive zone model) to simulate the interfacial delamination processes induced by a wedge indentation. In the traction-separation law, interfacial properties can be well described by two parameters: interfacial strength, σ_{strength}, which is the peak traction (stress) to separate an interface, and interfacial energy, Γ_0, which is the work-of-separation per unit area of the interface [22,23]. An advantage of using the traction-separation law is that it is not necessary to make assumptions that interfaces are fully bonded, fully debonded, or pre-cracked, since interfacial delamination criterion is inherently included in the traction-separation law. Thus, it can capture and predict onset and propagation of interfacial delamination. By combining the traction-separation law and finite element method, deformation of a ductile thin film, which was adhesively bonded to a ductile substrate during a wedge indentation, was simulated for the diversity of interfacial properties and thin film thicknesses [21]. An indentation P–*h* curve was obtained through the simulations. At onset of interfacial delamination, there was a significant load reduction, which was defined as a critical indentation load P_c for interfacial delamination. Generally speaking, this simulation is a direct approach, i.e. with assumed interfacial strength and interfacial energy values to derive a *P–h* curve, so that the interfacial delamination is characterized by a critical indentation load at the indentation *P–h* curve. On the other hand, the reverse problem, i.e. determining the interfacial properties from a known *P–h* curve, is more interesting and technically important. However, it is not

possible to determine two interfacial quantities (interfacial strength, $\sigma_{strength}$, and interfacial energy, Γ_0) based on a single critical indentation load alone at the onset of delamination. Recently, Li and Siegmund [24,25] also used the traction-separation law to simulate the interfacial properties of a thin-film/substrate system using conical indentation tests. They proposed a scheme to determine the two characteristic interfacial properties based on the two indentation loads on the nano-indentation P–h curves, i.e. a critical load, P_c, at onset of the interface delamination, and an additional indentation load, P_d, at an additional penetration depth d after the interface delamination. Both P_c and P_d are functions of the interfacial strength, $\sigma_{strength}$, and interfacial energy, Γ_0; therefore, the two interfacial quantities can be determined through the indentation experiments by knowing these two indentation loads. However, the additional penetration depth d in this method is somewhat arbitrary. Consequently, the interfacial adhesion properties may not be evaluated precisely.

Following previous studies [19–21], this paper presents a new scheme to determine the two characteristic interfacial parameters from the nano-indentation P–h curves based on indentations with two wedge tips. The new scheme is applied to determine the interfacial properties of two technologically important low dielectric constant (k) films: BlackDiamond (BD)/Si and methylsilsesquioxane (MSQ)/Si systems. In this method, the interfacial delamination processes by wedge indentations (wedge inclusion angles of 90° and 120°) are simulated using finite element software [26] in combination with the traction-separation law [22,23]. Based on FEM simulations, relationships between the critical indentation loads at onset of interfacial delamination (the critical load with the wedge tip of 90° inclusion angle, P_c^{90}, and the critical load with the wedge tip of 120° inclusion angle, P_c^{120}) and the interfacial adhesion properties of the thin-film/substrate systems are established. The critical indentation loads are found to be functions of the indenter angles and the interfacial properties. However, for a particular thin-film/substrate system, the interfacial strength and interfacial energy are fixed values and should be independent of the indenter tips used. Therefore, it is possible to use the two critical indentation loads (P_c^{90} and P_c^{120}) obtained from the wedge indentation experiments and the relationships developed from FEM simulations to determine the two interfacial quantities, and the results should be unique. Finally, the values of interfacial energy for the BD/Si and MSQ/Si systems obtained from the simulation are compared with reported experimental interfacial toughness values [19,20].

2. Wedge indentation experiments and finite element simulation

This study is divided into two parts: FEM simulation and wedge indentation experiments. In the experiments, a 500-nm thick BD film and 400-nm thick MSQ film, same as those used in previous studies [19,20], are used to determine the interfacial properties. A nano-indentation system (UMIS-2000H®, CSIRO, Canberra, Australia) is used for the experiments. Two wedge tips with inclusion angles of 90° and 120° are used. The lengths of the 90° wedge tip and 120° wedge tip are 4.06 and 4.21 μm, respectively. The wedge indentation tests consist of three main segments: (a) loading to the predefined maximum load in 20 s, (b) holding for 5 s at

Table 1. Material properties of film and substrate.

	E (GPa)	Poisson's ratio ν	Yielding strength, σ_y (GPa)	Strain-hardening exponent N
BD	12.6	0.34	1.47	0.25
MSQ	4.69	0.34	0.45	0.25
Substrate	112.4	0.28	3.10	N/A

the maximum load, and (c) unloading to 30% of the maximum load in 8 s. During the indentation, complete film delamination occurs around the indentation sites. For the BD film, the critical indentation load, P_c, is defined as the pop-in load at the P–h curves, i.e. a sudden increase in penetration depth during indentation at an approximately constant load [19]. For the MSQ film, the critical indentation load is higher than the pop-in load at the indentation load–displacement curve [20].

FEM simulations of wedge indentations are performed with the BD/Si and MSQ/Si system properties listed in Table 1. It is worth noting the differences between the experiments and simulations, as it might affect the accuracy of the proposed scheme. Firstly, the FEM simulations are done with a displacement control, whereas the experiments are done with a load control. When an interfacial delamination occurs, a loading control experiment will result in a large displacement change at an approximately constant load (known as pop-in); whereas a displacement control experiment will lead to a load reduction at an approximately constant displacement. Secondly, FEM simulation shows only interfacial delamination during indentation, whereas experiments show film cracking prior to interfacial delamination [19,20]. Since cracking in film is very difficult to simulate by the FEM method, the simulation does not include film cracking. Finally, the FEM simulation of wedge indentation is assumed a two-dimensional plane strain condition, i.e. the length of the wedge tip is infinite during the simulation; however, in the experiments, the wedge tips have fixed lengths, which may deviate from the pure plane strain condition.

3. Finite element analysis

3.1. *Cohesive zone model*

In the FEM simulations, both thin film and substrate are modeled as elasto-plastic materials based on the J_2 theory, and the stress–strain relation is

$$\varepsilon = \begin{cases} \sigma/E & \sigma \le \sigma \\ (\sigma_y/E)(\sigma/\sigma_y)^{1/N} & \sigma \le \sigma \end{cases}, \tag{1}$$

where σ_y is the yield strength, and N is the strain-hardening exponent.

The traction-separation law proposed by Tvergaard and Hutchinson [22,23] is used to simulate the interface separation process. A typical form of the traction-separation law is shown in Figure 1, where δ_n and δ_t are the separations in tangential and normal directions, respectively, δ_n^c and δ_t^c are two quantities that represent the critical separations in these two directions, and λ^c is the parameter to adjust the shape

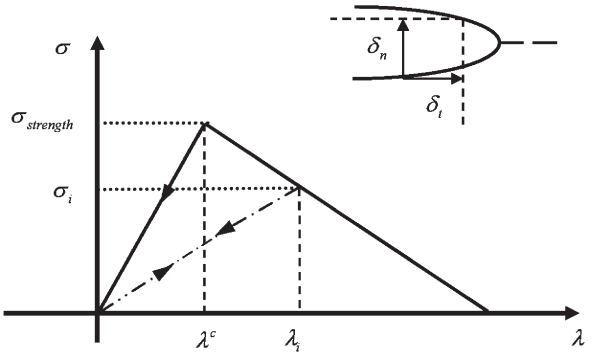

Figure 1. Schematic diagram showing a traction-separation law.

of the traction-separation law. σ_{strength} is the interfacial strength for the initiation of delamination, and the interfacial energy Γ_0 is the energy consumed by interface separation per unit area during the delamination process. Note that this form of traction-separation law is slightly different from that originally proposed by Tvergaard and Hutchinson [22,23], and is built in the ABAQUS software since version 7.5 [26].

Using the traction-separation law, one can define

$$\lambda = \sqrt{\left(\frac{\delta_n}{\delta_n^c}\right)^2 + \left(\frac{\delta_t}{\delta_t^c}\right)^2}, \tag{2}$$

where $\lambda = \lambda^c$ is the condition for onset of delamination, where λ^c is the critical separation at damage initiation, and the stress can be expressed as

$$\sigma(\lambda) = \begin{cases} \sigma_{\text{strength}}\lambda/\lambda^c & 0 < \lambda \le \lambda^c \\ \sigma_{\text{strength}}(1-\lambda)/(1-\lambda^c) & \lambda^c < \lambda \le 1. \end{cases} \tag{3}$$

The interfacial energy can be expressed as

$$\Gamma_0 = \frac{\sigma_{\text{strength}}\delta_n^c}{2}. \tag{4}$$

When the mixed-mode fracture energy criterion, $G_n + G_s + G_t = \Gamma_0$, is satisfied, complete failure occurs. The quantities G_n, G_s, and G_t refer to the work done by the traction and its conjugate relative displacement in the normal, the first and the second shear directions, respectively; hence, the interfacial energy is independent of the cracking mode.

As shown in Figure 1, if the effective normalized displacement separation is less than the critical value, $\lambda < \lambda^c$, the cohesive zone law remains reversible. For $\lambda > \lambda^c$, an irreversible unloading path is used so that unloading occurs linearly toward the origin of the traction-separation plane, as described by

$$T = \frac{T_i}{\lambda_i}\lambda = \frac{\sigma_i}{\lambda_i}\lambda, \tag{5}$$

where T_i and λ_i are the resulting traction and effective normalized separations at the point where unloading starts.

3.2. *A typical case by finite element simulation*

Considering an indentation of a typical film/substrate system, as illustrated in Figure 2, the indenter has a wedge-shaped tip with an inclusion angle, θ; due to its symmetry along the y-axis, only half of the system is modeled (2-D model). All parameters in the governing equations and the constitutive relations are normalized by a yield strength of the film, σ_{yf}, and a convenient length, $\Delta_0 = 1\,\mu m$. The geometric values for the thin-film/substrate system (see Figure 2) are: the thicknesses of the film and substrate are $h_f = 0.5\Delta_0$ and $h_s = 40\Delta_0$ respectively; and the width of the system is taken to be $L_s = 100\Delta_0$. In this paper, we only present the simulations for the thin films where both elastic modulus and hardness are lower than those of the substrate (Table 1), known as a soft-film-on-hard-substrate (SFHS) system. The properties of the BD and MSQ films are used as film properties in the simulations. The substrate is assumed to have properties similar to those of silicon, and the yield strength of the substrate is estimated from its hardness values. The wedge indenters are assumed as rigid bodies with inclusion angles of 90° and 120°, respectively. The shape of the traction-separation law and interfacial adhesion properties are defined as follows (see Equation (4)): $\lambda^c = 0.05$, $\delta_n^c/\delta_t^c = 1$. Interfacial strength values are varied in the range of $\sigma_{\text{strength}}/\sigma_{yf} = 0.2$–$0.8$, whereas the interfacial energy values vary within the range of $\Gamma_0/(\sigma_{yf}\Delta_0) = 2 \times 10^{-3} - 10 \times 10^{-3}$.

FEM simulations are performed using the commercial software ABAQUS [26]. The interface is modeled with 185 two-dimensional (2D) cohesive elements with four nodes and two integration points (COH2D4). The film and substrate are modeled with 6065 four-node two-dimensional (2D) bilinear-plane-strain-continuum-elements (CPE4). Small element size ($l = t/10$) is used in the area near the indenter, and the element size gradually increases with distance from the indenter, with a ratio 5 in the x-direction and 2.5 in the y-direction (Figure 2). The frictionless contact has been used for modeling the interaction between the wedge indenter tip and the film. The maximum indentation depth during simulation is maintained at less than the film thickness; in this way, the plastic deformation occurs only within the film. As the

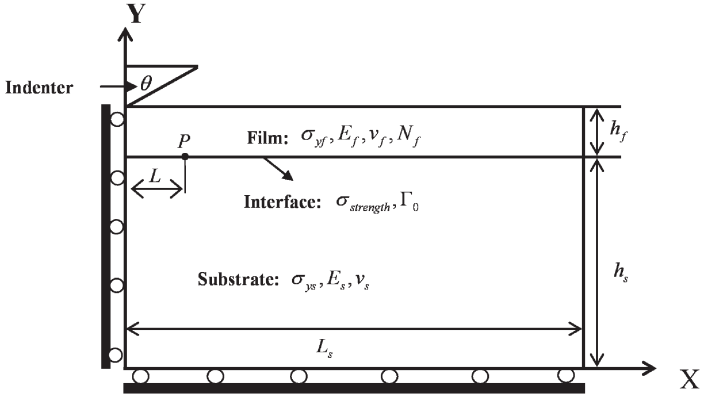

Figure 2. Schematic diagram showing the geometry of wedge indentation and material properties used in the FEM simulation.

yield strength of the substrate is very high, during the simulation, the substrate deforms elastically and no plastic deformation occurs in the substrate. These conditions are based on experimental observations reported previously [19,20]. In the previous studies, substrate plastic deformation was not observed during wedge indentation, as the indentation depth was less than the film thickness [19,20]. Therefore, the strain-hardening exponent for the substrate is not used in the simulation. In addition, the effects of mesh size on wedge indentation curves are insignificant and, therefore, not included in this paper.

Representative of the computations performed using the initial values given above, Figure 3 shows the indentation deformation, plastic zone, interfacial delamination and buckling for a SFHS system with interfacial properties of $\sigma_{\text{strength}}/\sigma_{yf} = 0.2$ and $\Gamma_0/(\sigma_{yf}\Delta_0) = 0.002$, plus an indentation penetration depth of $h_{\text{penetration}} = h - h_{se} = 0.8h_f$, where h is the indenter penetration depth and h_{se} is the substrate deformation depth. The plastic zone is characterized by the condition that the indentation-induced stress is higher than the yield strength of the film. During indentation delamination, as the indentation depth increases, the delamination crack length and radial stresses induced by the indenter simultaneously increase, causing a large radial displacement of the plastic zone within the film. Meanwhile, the deformation within the substrate remains small and elastic. Figure 3 also shows that the entire delamination crack is located within the plastic zone; this confirms the large-scale yielding caused by delamination during wedge indentation.

FEM simulations give the indentation P–h curve combined with the critical load and displacement at onset of delamination. Figure 4a shows the P–h curves of a

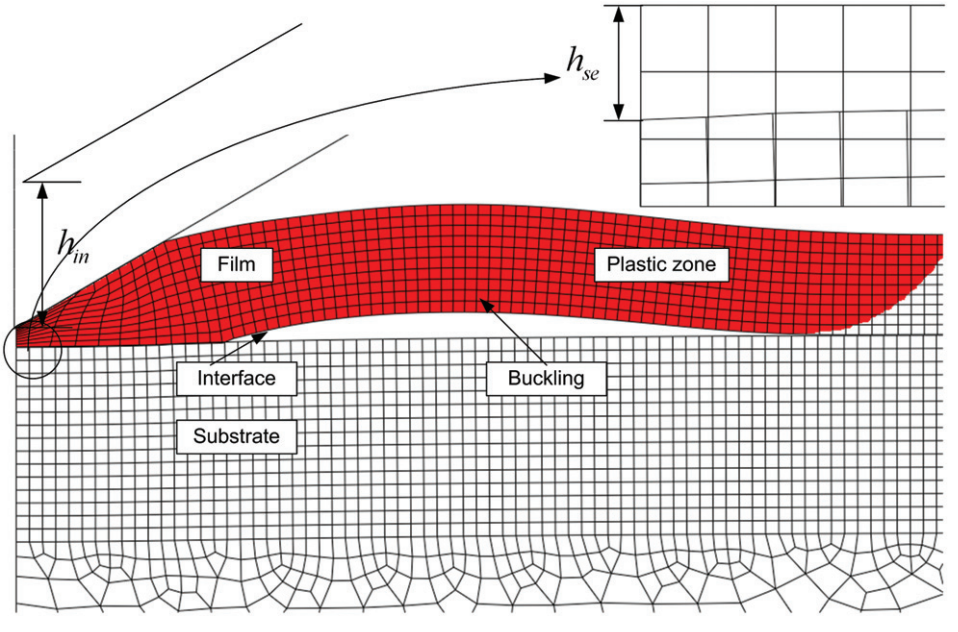

Figure 3. Contour of the plastic zone for the BD/Si system with $\sigma_{\text{strength}}/\sigma_{yf} = 0.2$ and $\Gamma_0/(\sigma_{yf}\Delta_0) = 0.002$ at an indentation depth of $h_{\text{penetration}} = h - h_{se} = 0.8h_f$.

SFHS system for a wedge tip with $\theta = 120^0$ for a range of interfacial strength values and a fixed interfacial energy value of $\Gamma_0/(\sigma_{yf}\Delta_0) = 0.01$. Figure 4b depicts the *P–h* curves for the same film system with a fixed interfacial strength value of $\sigma_{\text{strength}}/\sigma_{yf} = 0.6$ but with a series of interfacial energy values. As can be seen, the initial part of the curve is almost linear; therefore, it is anticipated that there is no substrate effect within this range of indentation depth. As the indentation depth increases, the curve becomes 'superlinear', i.e. the slope of the curve increases with indentation depth, most likely due to the increasing effect from the substrate. Since the substrate is stiffer than the film, the slope of the curve increases correspondingly. It is also found that, for all interfacial properties used, there is a sudden load decrease in the indentation *P–h* curve (Figure 4). This sudden load decrease corresponds to the onset of interfacial delamination, which defines a critical indentation load, P_c, for interfacial delamination. After delamination, the stiffness of the film/substrate system decreases significantly, which is clear from the further decreases in the slope of the curve. This can be understood as interfacial cracking (delamination) degrading the stiffness of the system.

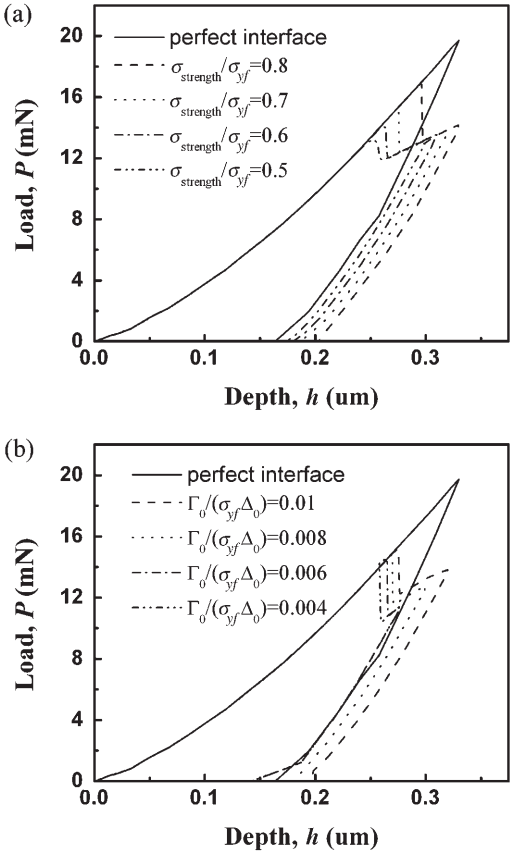

Figure 4. Load–indentation depth curves of the BD/Si system for: (a) a range of values of interfacial strength with a fixed interfacial energy of $\Gamma_0/(\sigma_{yf}\Delta_0) = 0.01$; (b) a range of values of interfacial energy with a fixed interfacial strength of $\sigma_{\text{strength}}/\sigma_{yf} = 0.6$.

3.3. *Parametric studies*

From the simulated P–h curve, the critical indentation load (P_c) for the onset of interfacial delamination can be determined. This critical indentation load is significantly affected by the interfacial energy (Γ_0) and interfacial strength (σ_{strength}), which govern the traction-separation law. It is, therefore, necessary to discuss the effects of these two parameters to the critical indentation load for the delamination.

3.3.1. *Effects of interfacial energy*

The effects of interfacial energy are studied by varying the values of interfacial energy at fixed values of interfacial strength as $\sigma_{\text{strength}} = 0.2\sigma_{yf}$, $0.6\sigma_{yf}$, $0.4\sigma_{yf}$, and $0.8\sigma_{yf}$. The normalized critical indentation loads, $P_c/(\sigma_{yf}\Delta_0)$, corresponding to the onset of interfacial delamination, as a function of interfacial energy, $\Gamma_0/(\sigma_{yf}\Delta_0)$, are shown in Figure 5a. As can be seen, for each fixed interfacial strength value, σ_{strength}, the critical indentation load increases approximately linearly with interfacial energy.

3.3.2. *Effects of interfacial strength*

When the interfacial energy, Γ_0, is fixed at a constant value, the critical load generally increases approximately in a fourth-order polynomial relation with increasing interfacial strength (Figure 5b). Comparing Figures 5a and b, it is found that interfacial strength influences critical indentation loads more significantly than that of interfacial energy. For example, for the SFHS system in the simulation, at the normalized interfacial strength of $\sigma_{\text{strength}}/\sigma_{yf} = 0.6$, increasing the normalized interfacial energy four-fold, from $\Gamma_0/(\sigma_{yf}\Delta_0) = 0.002$ to 0.008, leads to an increase in the normalized critical indentation load, $P_c/(\sigma_{yf}\Delta_0)$, from approximately 7.8 to 8.6 (Figure 5a). However, for the same film, if the interfacial energy is fixed at $\Gamma_0/(\sigma_{yf}\Delta_0) = 0.008$, increasing the interfacial strength by four times, i.e. from 0.2 to 0.8, leads to the critical indentation load, $P_c/(\sigma_{yf}\Delta_0)$, changes from approximately 5.0 to 15.0 (Figure 5b).

This parametric study indicates that critical indentation loads for onset of delamination scales predominately with interfacial strength. This is because during wedge indentation, the total energy dissipation is closely related to the plastic energy dissipation arising from plastic deformation and surface energy arising from interface delamination. It appears that, if the ratio of $\sigma_{\text{strength}}/\sigma_{yf}$ is larger than 0.4, increasing interfacial strength would cause a more significant increase in plastic deformation than that increasing interfacial energy, resulting in a more significant increase in critical indentation loads. Furthermore, the parametric studies suggest that the critical indentation load for onset of delamination has the following functional form with interfacial strength and interfacial energy:

$$P_c = f\left(\sigma^n_{\text{strength}}, \Gamma_0\right). \tag{6}$$

The exact form of Equation (6) needs further study; a simple form can be considered as $n = 4$, and this will be discussed in Section 4.1.

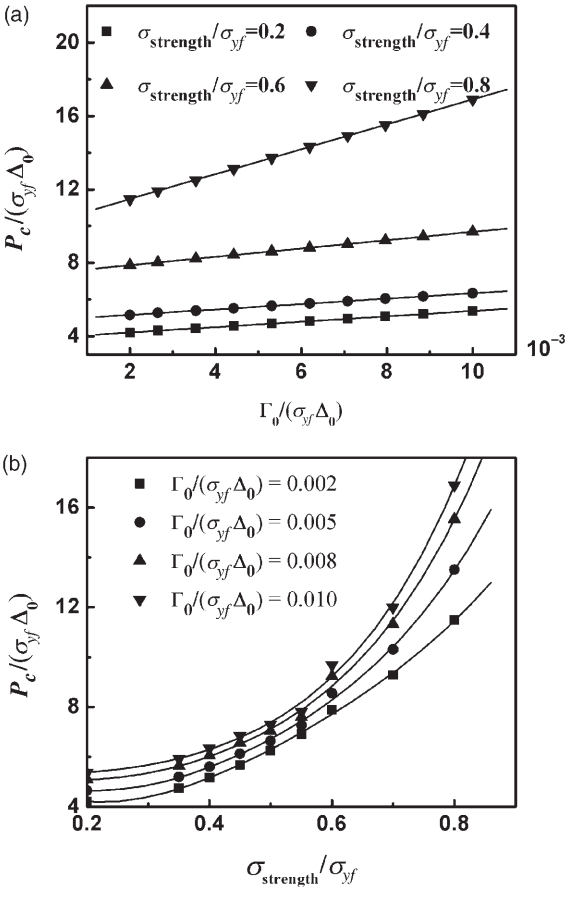

Figure 5. Normalized critical indentation load $P_c/(\sigma_{yf}\Delta_0)$ (μm) for the BD/Si system versus (a) normalized interfacial energy $\Gamma_0/(\sigma_{yf}\Delta_0)$ at a range of interfacial strength (the solid lines are the linear fit of the data points); (b) normalized interfacial strength $\sigma_{strength}/\sigma_{yf}$ at a range of interfacial energy (the solid lines are the fourth-order polynomial fit of the data points).

3.4. *Mode mixity*

Within the cohesive zone model, the mode mixity is quantified by the mode mix of the normal and shear deformation fields as

$$\tan\psi_{cz} = \left(\frac{\delta_t}{\delta_n}\right). \tag{7}$$

The FEM simulation indicates that before interfacial delamination, normal traction along the interface has a negative value, which means that the film and substrate are in contact. Correspondingly, the normal separation is zero along the interface; therefore, the interface is subjected to a pure shear mode.

However, after interfacial delamination and further propagation of the interfacial crack, at a load higher than the critical indentation load, shear traction decreases and

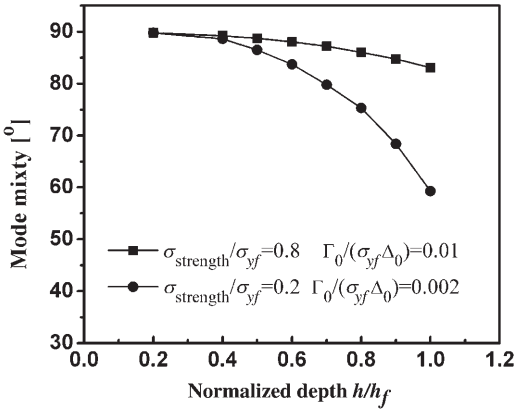

Figure 6. Dependence of mode mixity on normalized indentation depth.

a bending moment appears. Thus, buckling occurs and the film lifts off the substrate. Hence, the normal separation U_y increases considerably faster than the shear separation U_x, and subsequently changes into a mixed mode upon further propagation, as shown in Figure 6. This result is consistent with that obtained by Li and Siegmund [25].

4. Interfacial properties

4.1. *Determination of interfacial properties*

Using conventional traction-separation law, a two-step process is usually needed to estimate the interfacial strength and interfacial energy. For example, for ductile crack growth, the cohesive energy was first obtained from the measured crack initiation toughness, and the tearing modulus was used to find the cohesive strength [23]. However, for most indentation problems, due to the large-scale yielding phenomenon, this two-step process can not be used [25].

The parametric studies presented in the Section 3.3 showed that increasing either interfacial strength ($\sigma_{strength}$) or interfacial energy (Γ_0) resulted in increases in critical indentation load (P_c) at the onset of interfacial delamination. Their relationships could be described approximately by either a linear or a fourth-order polynomial fitting function. The surface plots of these numerical relations for 90° and 120° wedge indentations in the SFHD system are shown in Figures 7a and b, respectively. However, the traction-separation law characterizes the interface with two parameters, i.e. interfacial strength and interfacial energy. Thus, one critical indentation load at onset of delamination cannot give the two unique values of the interfacial properties. To determine the two parameters from the *P–h* curves, two critical data points are needed. In this work, the interfacial delamination processes of the thin-film/substrate system by indentations with 90° and 120° wedge tips, respectively, are modeled with the same material properties and traction-separation law parameters at the interface. The critical indentation loads for a wedge tip of 90° inclusion angle, P_c^{90}, and for a wedge tip of 120° inclusion angle, P_c^{120} can be obtained

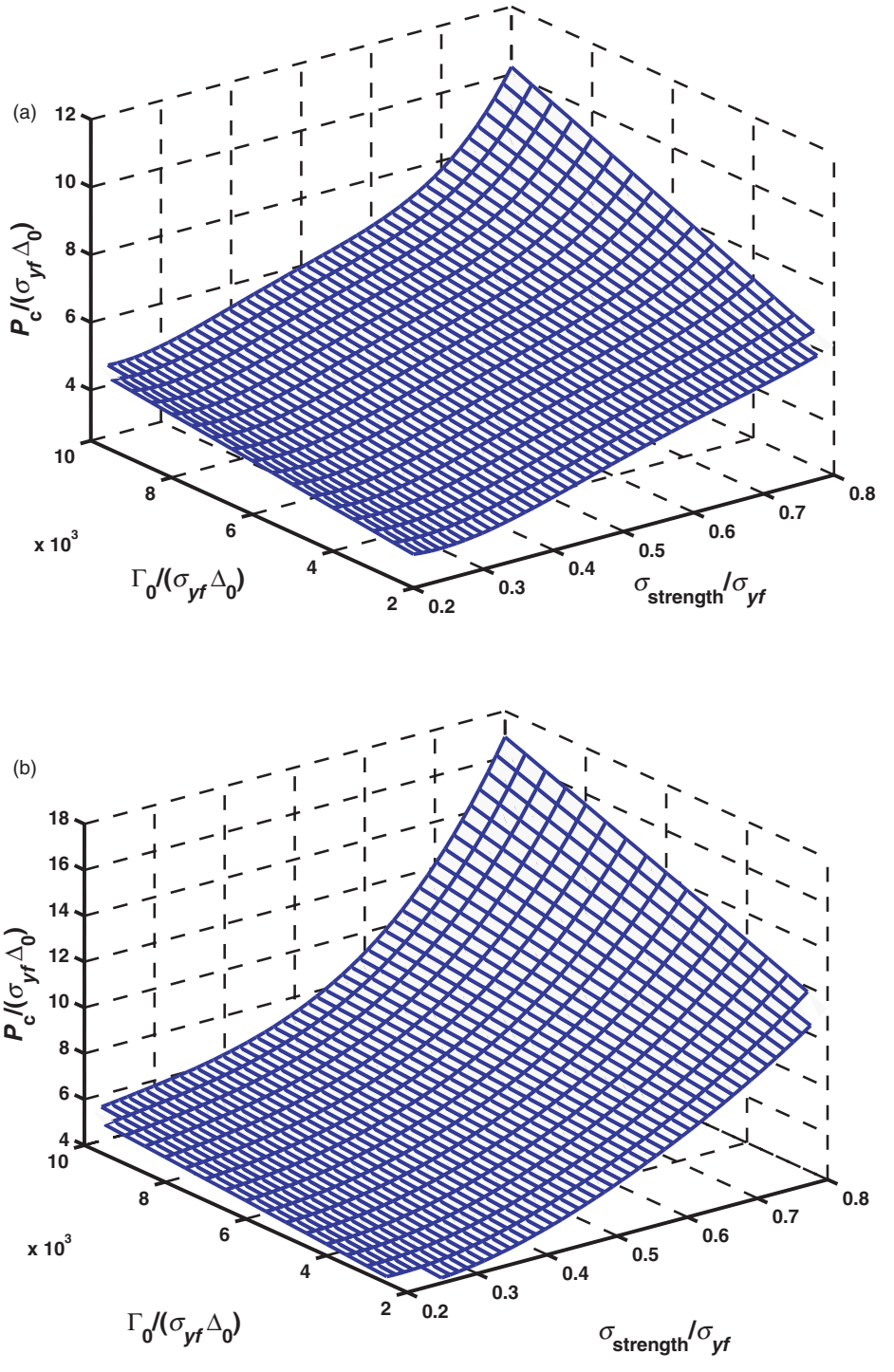

Figure 7. Surface plots of the dependence of interfacial adhesion properties versus (a) normalized critical indentation load with 90° indenter, $P_c^{90}/(\sigma_{yf}\Delta_0)$ (μm); (b) normalized critical indentation load with 120° indenter, $P_c^{120}/(\sigma_{yf}\Delta_0)$ (μm), for the BD/Si system.

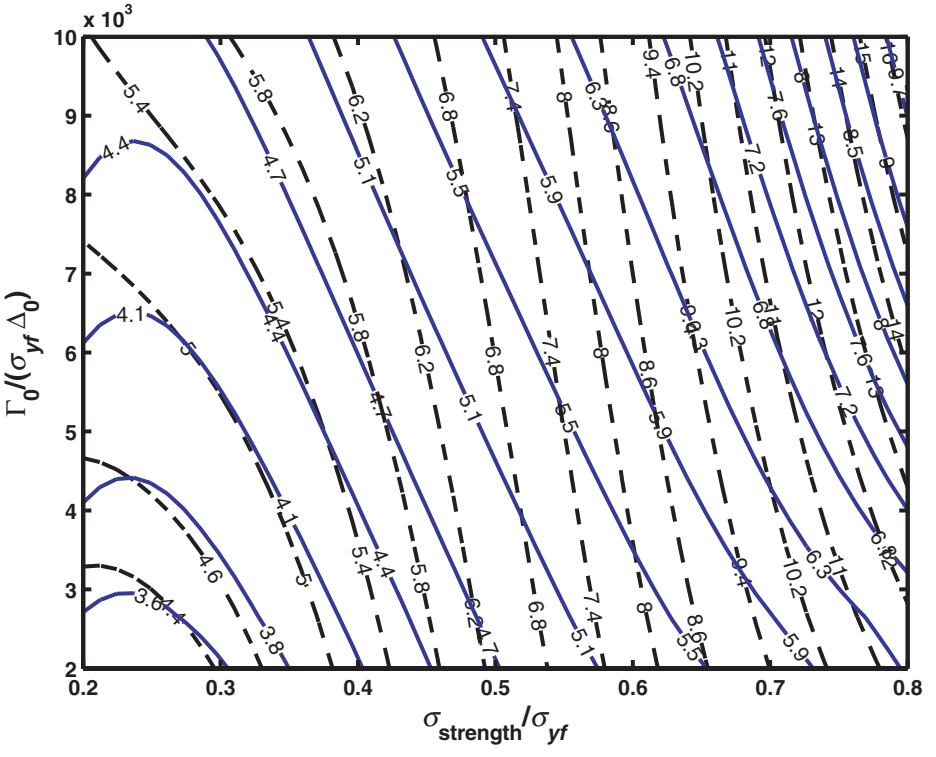

Figure 8. Contour plots of the variation in normalized P_c^{90} and $P_c^{120}$for the BD/Si system (solid lines: $P_c^{90}/(\sigma_{yf}\Delta_0)$ (μm) and dashed lines: $P_c^{120}/(\sigma_{yf}\Delta_0)$ (μm).

from the simulated *P–h* curves. These two critical indentation loads can then be used as two characteristic parameters (Figure 7). By re-plotting the data in Figure 7, one can obtain the interface energy-strength contour plot for SFHS system, as shown in Figure 8. For each pair of critical indentation load data: $[P_c^{90}/(\sigma_{yf}\Delta_0); P_c^{120}/(\sigma_{yf}\Delta_0)]$, a pair of intersecting lines can be found in the interface energy–strength contour plots. The coordinates of the intersection point give the normalized cohesive zone properties ($\Gamma_0/(\sigma_{yf}\Delta_0)$ and $\sigma_{\text{strength}}/\sigma_{yf}$), which can be used to determine the interfacial properties of the film/substrate systems.

4.2. *Proposed scheme for interfacial properties determinations*

From the contour plot (Figure 8), we can now propose a scheme to determine the interfacial adhesion properties from wedge indentation *P–h* curves, which can be summarized as follows:

(1) First, it is necessary to determine the elastic–plastic properties of the thin film and substrate required for FEM simulation. The elastic modulus and hardness of the thin film can be determined by normal indentation with a standard Berkovich indenter tip. However, the yield strength and strain

hardening exponential of the thin films cannot be determined directly through the indentation experiment. For wedge indentation, Johnson's analysis [27] can be used to estimate the yield strength after acquiring the elastic modulus and hardness of the film. The values of yield strength and the strain-hardening exponential can be adjusted by matching the simulation and experiment curves before the onset of interfacial delamination. It is assumed that the simulated and experimental curves can be matched for the sections of the curves prior to interfacial delamination and film cracking. These sections of the curves should only be related to the indentation elastic–plastic deformation, as they are performed with different control modes (load-control in experiments and displacement control in simulation). Figure 9 shows that the simulated and experimental indentation P–h curves are well matched before the onset of interfacial delamination (simulation) and film cracking (experiments) for both BD and MSQ films.

(2) FEM simulations of wedge indentation with two tips having different inclusion angles (preferably 90° and 120°) for the initial interfacial adhesion properties are performed and indentation P–h curves obtained from the simulation. The critical indentation loads for the onset of delamination can be found from the curves.

(3) A series of FEM simulations are then performed to obtain the dependence of the two critical indentation loads P_{cs}^{90} and P_{cs}^{120} on the values of interfacial strength σ_{strength} and interfacial energy Γ_0. The results will form an interface energy–strength contour plot, such as that shown in Figure 8.

(4) Indentation experiments are conducted using the wedge tips with two inclusion angles (90° and 120°) and the values of the critical indentation loads for the onset of delamination, P_c, are obtained from the experimental P–h curves. The experimentally obtained P_c^{90} and P_c^{120} from the P–h curves are plotted into the interface energy–strength contour plots, and from the intersection point of the two curves, the interfacial strength, σ_{strength}, and interfacial energy, Γ_0, can be extracted.

In this paper, the simulation results are normalized with the respective yield strength of the film; therefore, this proposed scheme for characterizing interfacial properties by wedge indentation is a general method and applicable for different thin-film/substrate systems as long as the film's elastic modulus and hardness are smaller than those of the substrate. For hard-film-on-soft-substrate, or where the film's elastic modulus is higher than that of the substrate, further simulations are needed. This work will be discussed separately and is not included in this paper.

4.3. *Applications of the proposed scheme*

4.3.1. *BD/Si system*

Figure 10a shows the calculated interface energy–strength contour for BD/Si system together with the experimentally obtained two critical indentation loads for onset of interface delamination. Unlike the experimental wedge indentation curves, the simulated curve does not include film cracking; therefore, the critical indentation load P_c may differ for the experiment and simulation. In the wedge indentation

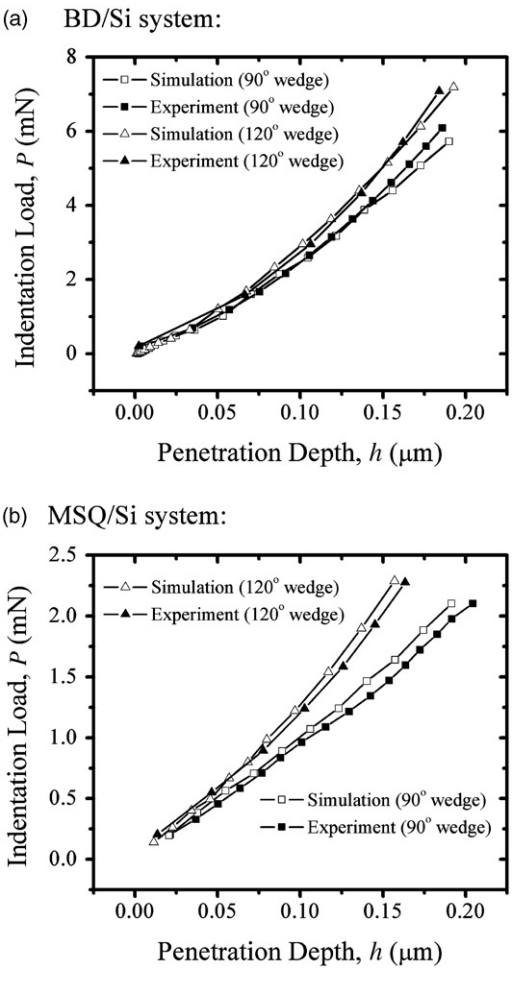

Figure 9. *P–h* curves before the occurrence of interfacial delamination for (a) the BD/Si system and (b) the MSQ/Si system. Open and filled triangle symbols represent the simulated and experimental curves of 120° wedge indentation, respectively. Open and filled square symbols represent the simulated and experimental curves of 90° wedge indentation, respectively.

experiments, the indentation load for interfacial delamination is usually higher than that for film cracking [19,20]; however, for BD film, the differences in the values of P_c are very small due to the brittle fractures in the BD film and at the interface occurring at approximately the same load [20]. In this study, it is assumed that P_c is equal to the pop-in load at the *P–h* curve; however, the pop-in load may vary as the fracture of the BD/Si system occurs in a brittle manner. It is found experimentally for the BD film that the critical loads for 90° wedge indentation are in the range of $P_c^{90} = 7.56 - 7.61$ mN, and $P_c^{120} = 9.66 - 10.16$ mN for 120° wedge indentation. In this study, a convenient length, $\Delta_0 = 1\,\mu$m, and film yield strength ($\sigma_y = 1.47$ GPa) are used to normalize all the properties. Therefore, the normalized critical indentation

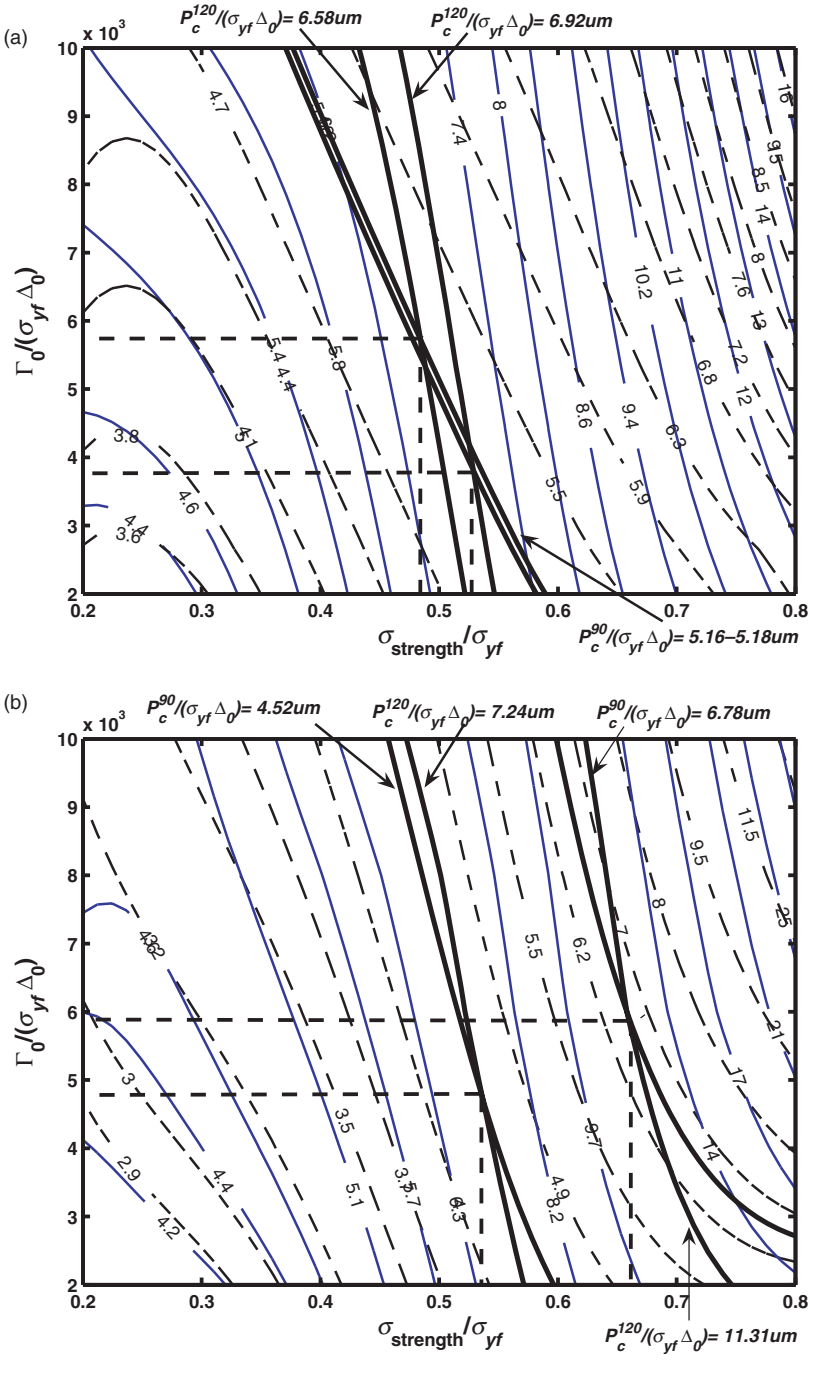

Figure 10. (a) BD/Si system's interface energy–strength contour for 90° and 120° wedge indentation showing the intersections of $P_c^{90}/(\sigma_{yf}\Delta_0) = 5.16$–$5.18\,\mu m$ and $P_c^{120}/(\sigma_{yf}\Delta_0) = 6.58$–$6.92\,\mu m$. Full lines represent the contour for $P_c^{90}/(\sigma_{yf}\Delta_0)$, while dashed lines represent that for $P_c^{120}/(\sigma_{yf}\Delta_0)$. (b) MSQ/Si system's interface energy–strength contour for 90° and 120° wedge indentation showing the intersection of $P_c^{90}/(\sigma_{yf}\Delta 0) = 4.52$–$6.78\,\mu m$ and $P_c^{120}/(\sigma_{yf}\Delta_0) = 7.24$–$11.31\,\mu m$. Filled lines represent the contour for $P_c^{90}/(\sigma_{yf}\Delta_0)$, while dashed lines represent that for $P_c^{120}/(\sigma_{yf}\Delta_0)$.

loads are calculated to be in the range of 5.16–5.18 μm for 90° wedge tip, and 6.58–6.92 μm for 120° wedge tip. The four curves corresponding to the minimum and maximum values of the critical indentation loads for 90° and 120° wedge indentations are then plotted in the contour plot shown Figure 10a; it is clear that there are four intersection points in the contour plot. As discussed in a previous study [19], the 90° and 120° wedge indentations tests on the same film system should yield the same interface properties, regardless of the difference in wedge indenter inclusion angles. Therefore, the interface properties of the same thin-film/substrate system should not change with indenter tip angles. Hence, from the four points of intersections between the curves of $P_c^{90}/(\sigma_{yf}\Delta_0) = 5.16$–$5.18\,\mu m$ and $P_c^{120}/(\sigma_{yf}\Delta_0) = 6.58$–$6.92\,\mu m$ in the contour plot (Figure 10a), the normalized interfacial energy $\Gamma_0/(\sigma_{yf}\Delta_0)$, and normalized interfacial strength $\sigma_{strength}/(\sigma_{yf}\Delta_0)$, for the BD/Si system can be determined. By replacing the values of σ_{yf} and Δ_0, it is found that the interfacial energy, $\Gamma_0 = 5.58$–$8.49\,J/m^2$, and interfacial strength, $\sigma_{strength} = 0.71$–$0.78\,GPa$, for the 500-nm BD film on Si substrate.

The interfacial adhesion energy obtained using the interface energy–strength contour in this study ($\Gamma_0 = 5.58$–$8.49\,J/m^2$) is higher than the interface toughness determined previously ($\Gamma_0 = 5.40 \pm 0.90\,J/m^2$) for the same 500 nm thick film [19,20]. There may be several reasons for this discrepancy, which will be discussed together with the results of the MSQ film in the next section.

4.3.2. *MSQ/Si system*

The interface energy–strength contour for the MSQ/Si system (Figure 10b) is also developed in this work using the film properties listed in Table 1. According to the fracture–indentation correlation study for the MSQ/Si system [19], pop-ins occurred at 2 and 3.25 mN for 90° and 120° wedge indentations, respectively. However, interfacial delamination occurred at 3 and 5 mN for the 90° and 120° wedge indentations, respectively. Assuming the latter values (3 and 5 mN) are critical indentation loads, $P_c^{90}/(\sigma_{yf}\Delta_0)$ and $P_c^{120}/(\sigma_{yf}\Delta_0)$ for the MSQ/Si system ($\sigma_{yf} = 0.45\,GPa$) can be calculated as 6.78 and 11.31 μm, respectively. From the intersection of these two curves [$P_c^{90}/(\sigma_{yf}\Delta_0) = 6.78\,\mu m$ and $P_c^{120}/(\sigma_{yf}\Delta_0) = 11.31\,\mu m$], the interfacial energy, Γ_0, is determined to be $2.61\,J/m^2$ and interfacial strength, $\sigma_{strength}$, is found to be 0.29 GPa. These can be considered as higher-bound values for the interfacial properties. The lower-bound values can be determined in a similar way using the pop-in loads (2 and 3.25 mN, respectively, for 90° and 120° indenter tips). The low-bound values are found to be $2.13\,J/m^2$ for Γ_0 and 0.24 GPa for $\sigma_{strength}$. The interfacial energy for the MSQ/Si system was previously determined to be $1.89 \pm 0.28\,J/m^2$ for the 90° wedge indentation and $1.92 \pm 0.08\,J/m^2$ for the 120° wedge indentation [19]. Note that the interfacial energy obtained from the contour plot is also higher than previous results for the MSQ/Si system, which is consistent with the finding for the BD/Si system. Nevertheless, these results have confirmed the validity of the method proposed in this study, which combines FEM simulation with actual experiment.

One possible reason that the values of Γ_0 determined from the contour plots are higher than previously reported values is differences in the interface crack-fronts between the experiments and FEM simulations. In the simulation, a 2-D plane strain

condition is assumed since the wedge is infinite in length. In the experiments, however, the wedge indenter length (approximately 4 μm) may not be long enough to achieve a complete plane strain condition, especially at the two ends of the wedge tips, where film cracking might alter the strain conditions and introduce some errors in the calculations [19]. Therefore, if a longer wedge tip is used, the differences of stress–strain conditions between the experiment and simulation may be less significant and the interfacial adhesion results would be more accurate. The effect of wedge indenter length will be the subject of further study.

Interfacial energy and strength values determined from the interfacial energy–strength contour plot are within a certain range for both BD/Si and MSQ/Si systems: $\Gamma_0 = 5.58$–$8.49\,\mathrm{J/m^2}$ and $\sigma_{\mathrm{strength}} = 0.71$–$0.78\,\mathrm{GPa}$ for the 500-nm BD film on Si substrate, and $\Gamma_0 = 2.13$–$2.61\,\mathrm{J/m^2}$ and $\sigma_{\mathrm{strength}} = 0.24$–$0.29\,\mathrm{GPa}$ for MSQ film on Si substrate. Interestingly, if one takes the average values of the interfacial energy in the above ranges, i.e. $\Gamma_{0,\mathrm{m}} = 7.04\,\mathrm{J/m^2}$ for the BD/Si and $\Gamma_{0,\mathrm{m}} = 2.37\,\mathrm{J/m^2}$ for MSQ/Si system, it is found that these values are approximately 25–30% higher than the interfacial toughness values determined previously for the same films [19,20]. These results suggest that there could be a constant in the previous empirical equation used to determine interfacial toughness from the wedge indentation of thin films [19,20]. This will be the subject of future studies.

Another possible reason is that the values of yield strength for the films are determined experimentally based on empirical relationships. There could be some errors in the values used for normalization, which can also introduce errors into the determination of interfacial properties.

Despite the differences, the interfacial adhesion properties determined in this study are consistent and similar to previously obtained experimental values [19,20]. Thus, the methodology proposed in this work is useful for the determination of interfacial mechanical properties based on wedge indentation experiments.

5. Summaries and conclusions

This paper presents a finite element simulation to determine the interfacial adhesion properties based on a traction-separation law and wedge indentation *P–h* curves. Traction-separation law inherently includes interface crack initiation and propagation criteria; therefore, eliminating the assumption that the interfaces are either fully bonded or pre-cracked. Moreover, the cohesive law accounts for energy dissipation during interface delamination and plastic zone separately; hence, FEM simulation based on traction-separation law is an effective way to solve large-scale yielding problems.

Based on the simulation work presented here, we propose a scheme combining FEM simulation and wedge indentation experiments to determine interfacial strength, $\sigma_{\mathrm{strength}}$, and interfacial energy, Γ_0, from the indentation *P–h* curves. Parametric studies on the dependence of critical indentation loads on interfacial strength and interfacial energy have led to the contour plot, which provides a bridge between the interfacial properties and the indentation *P–h* curves. From the contour plots of the BD/Si and MSQ/Si systems, the critical loads of the 90° and 120° wedge-indentation experiments have been numerically translated into their respective

interfacial energy and interfacial strength with good precision. In conclusion, this study has provided a numerical solution to the wedge indentation-induced delamination problem and the results are comparable to those obtained in previous experimental work [19,20].

Acknowledgement

This work was supported by National University of Singapore under Academic Research Funds (R265-000-190-112 and R265-000-190-133).

References

[1] A.A. Volinsky, N.R. Moody and W.W. Gerberich, Acta Mater. 50 (2002) p.441.
[2] M.D. Kriese, D.A. Boismier, N.R. Moody and W.W. Gerberich, Eng. Fract. Mech. 61 (1998) p.1.
[3] M. Lane, Annu. Rev. Mater. Res. 33 (2003) p.29.
[4] Y.G. Wei and J.W. Hutchinson, Int. J. Fract. 93 (1998) p.315.
[5] J. Malzbender, J.M.J. den Toonder, A.R. Balkenende and G. de With, Mater. Sci. Eng. A 36 (2002) p.47.
[6] A.A. Volinsky and W.W. Gerberich, Microelectron. Eng. 69 (2003) p.519.
[7] A.A. Volinsky, J.B. Vella and W.W. Gerberich, Thin Solid Films 429 (2003) p.201.
[8] M.D. Kriese, W.W. Gerberich and N.R. Moody, J. Mater. Res. 14 (1999) p.3007.
[9] M.D. Kriese, W.W. Gerberich and N.R. Moody, J. Mater. Res. 14 (1999) p.3019.
[10] D.B. Marshall and A.G. Evans, J. Appl. Phys. 56 (1984) p.2532.
[11] C. Rossington, A.G. Evans, D.B. Marshall and B.T. Khuri-Yakub, J. Appl. Phys. 56 (1984) p.2639.
[12] M.V. Swain and J. Menčik, Thin Solid Films 253 (1994) p.204.
[13] M.D. Drory and J.W. Hutchinson, Proc. R. Soc. Lond. A 452 (1996) p.2319.
[14] M.P. De Boer and W.W. Gerberich, Acta Mater. 44 (1996) p.3169.
[15] M.P. De Boer and W.W. Gerberich, Acta Mater. 44 (1996) p.3177.
[16] J.J. Vlassak, M.D. Drory and W.D. Nix, J. Mater. Res. 12 (1997) p.1900.
[17] M.R. Begley, D.R. Mumm, A.G. Evans and J.W. Hutchinson, Acta Mater. 48 (2000) p.3211.
[18] M. Schulze and W.D. Nix, Int. J. Solid. Struct. 37 (2000) p.1045.
[19] K.B. Yeap, K.Y. Zeng, H.Y. Jiang, L. Shen and D.Z. Chi, J. Appl. Phys. 101 (2007) p.123531.
[20] K.B. Yeap, K.Y. Zeng and D.Z. Chi, Acta Mater. 56 (2008) p.977.
[21] Y.W. Zhang, K.Y. Zeng and R. Thampurun, Mater. Sci. Eng. A 319/321 (2001) p.893.
[22] V. Tvergaard and J.W. Hutchinson, Phil. Mag. A 70 (1994) p.641.
[23] V. Tvergaard and J.W. Hutchinson, Int. J. Solid. Struct. 33 (1996) p.3297.
[24] W. Li and T. Siegmund, Acta Mater. 52 (2004) p.2989.
[25] W. Li and T. Siegmund, Comput. Model. Eng. 5 (2004) p.81.
[26] ABAQUS User Manual, version 7.5, Simulia, Providence, RI, 2007.
[27] K.L. Johnson, J. Mech. Phys. Solid. 18 (1970) p.115.